

Drug-Eluting Stent Design is a Determinant of Drug Concentration at the Endothelial Cell Surface

TAEWON SEO,¹ ANTOINE LAFONT,^{2,3} SUN-YOUNG CHOI,⁴ and ABDUL I. BARAKAT³

¹School of Mechanical Engineering, Andong National University, Andong, Korea; ²Department of Cardiology, European Georges Pompidou Hospital, University of Paris-Descartes, Paris, France; ³Hydrodynamics Laboratory (LadHyX), CNRS UMR7646, Ecole Polytechnique, Route de Saclay, 91128 Palaiseau Cedex, France; and ⁴Department of Radiology and Medical Research Institute, School of Medicine, Ewha Womans University, Seoul, Korea

(Received 9 July 2015; accepted 2 December 2015; published online 28 January 2016)

Associate Editor Peter E. McHugh oversaw the review of this article.

Abstract—Although drug-eluting stents (DES) have greatly reduced arterial restenosis, there are persistent concerns about stent thrombosis. DES thrombosis is attributable to retarded vascular re-endothelialization due to both stent-induced flow disturbance and the inhibition by the eluted drug of endothelial cell proliferation and migration. The present computational study aims to determine the effect of DES design on both stent-induced flow disturbance and the concentration of eluted drug at the arterial luminal surface. To this end, we consider three closed-cell stent designs that resemble certain commercial stents as well as three “idealized” stents that provide insight into the impact of specific characteristics of stent design. To objectively compare the different stents, we introduce the Stent Penalty Index (SPI), a dimensionless quantity whose value increases with both the extent of flow disturbance and luminal drug concentration. Our results show that among the three closed-cell designs studied, wide cell designs lead to lower SPI and are thus expected to have a less adverse effect on vascular re-endothelialization. For the idealized stent designs, a spiral stent provides favorable SPI values, whereas an intertwined ring stent leads to an elevated SPI. The present findings shed light onto the effect of stent design on the concentration of the eluted drug at the arterial luminal surface, an important consideration in the assessment of DES performance.

Keywords—Drug-eluting stent, Endothelial wound healing, Convection–diffusion, Wall shear stress, Flow disturbance, Computational simulations.

Address correspondence to Abdul I. Barakat, Hydrodynamics Laboratory (LadHyX), CNRS UMR7646, Ecole Polytechnique, Route de Saclay, 91128 Palaiseau Cedex, France. Electronic mails: Abdul.Barakat@ladhyx.polytechnique.fr and barakat@ladhyx.polytechnique.fr

INTRODUCTION

The clinical use of drug-eluting stents (DES) that release anti-proliferative agents into the arterial wall has greatly reduced the incidence of vascular occlusive restenosis observed with the deployment of bare metal stents (BMS).^{7,30,40} There are persistent concerns, however, about stent thrombosis in DES patients.^{7,27,31,35} Although relatively rare, stent thrombosis is associated with high mortality rates when it occurs. This has motivated continued interest in the safety of DES and their clinical efficacy relative to both BMS and other interventional procedures including coronary artery bypass surgery.

Although the mechanisms governing the occurrence of stent thrombosis following DES deployment remain incompletely understood, it is likely that hampered or retarded vascular re-endothelialization is centrally involved. Deployment of a stent at an arterial site massively damages the endothelium at that site,^{38,39,45} and sufficiently rapid repair of this endothelial injury is critical for the success of a stenting procedure. In the case of BMS, the stent struts become embedded in the arterial wall within a few weeks, and the stented region gets covered with new endothelium.²³ In the case of DES, on the other hand, there is evidence of prolonged in-stent inflammation and stunted re-endothelialization which leaves the stent struts exposed directly to blood flow for longer periods of time and increases the likelihood of in-stent thrombotic events.^{13,23,27}

Arterial re-endothelialization post-stenting requires endothelial cell proliferation and migration into the wounded area. In addition to preventing smooth

muscle cell proliferation and neointimal formation, drugs used in DES also have an anti-proliferative effect on vascular endothelial cells,^{34,45} which retards vascular wound healing. Therefore, it is desirable for drug concentration at the endothelial cell surface to be minimized while simultaneously ensuring that the concentration at the smooth muscle cell surface is sufficiently high to produce the required therapeutic effect. Despite the tendency in more recent DES designs to apply the drug coating only to the abluminal aspect of the stent, many stents in use today continue to have drug coating over the entire stent surface; therefore, a portion of the eluted drug in those designs is released directly into the lumen where it is rapidly convected by blood flow.²⁸ Several studies have investigated drug release from DES^{24,26} and its subsequent transport within the arterial wall.^{6,25,28,36,44} However, less is known about the effect of the portion of the drug that is released into the bloodstream where it can come in direct contact with endothelial cells within and immediately downstream of the stent and thus influence the proliferation and migration rates of these cells. Therefore, there is a need to establish if drug concentrations on the endothelial luminal surface in the vicinity of a stent are high and if so, to devise methods for minimizing these concentrations.

An additional factor affecting endothelial wound healing is the local hemodynamic environment. Blood flow-derived mechanical forces, particularly fluid dynamic shear stress, regulate endothelial structure and function including cell proliferation and migration rates.^{1,9,10,15,16} Various studies have demonstrated that placement of a stent within an arterial segment perturbs the local flow field significantly due to partial protrusion of stent struts into the flow field.^{4,5,8,17,22,33,41} While this effect is short-lived in the case of BMS that become rapidly embedded in the arterial wall, it is longer-lasting for DES. The nature of stent-induced flow disturbance depends intricately on stent design, most notably on stent strut thickness and spacing as well as the orientation of stent strut connectors relative to the flow direction.^{3,11,12,33,41} Therefore, different stent designs are associated with different degrees of flow disturbance. When it occurs, flow disturbance often takes the form of flow separation and recirculation zones within which wall shear stresses are generally low. This is significant in light of *in vivo* and *in vitro* data showing that low shear stress levels are associated with impaired endothelial wound healing as well as increased incidence of occlusive restenosis.^{1,15,16,45,46} More generally, different stent designs have also been shown to be associated with different rates of restenosis.^{19,20,29,32,38}

In light of the above, the performance of DES is expected to be improved by minimizing both the drug concentration at the endothelial cell surface and the

extent of stent-induced flow disturbance. Importantly, these two effects are coupled because the concentration of the eluted drug within the flow field, and hence on the surface of endothelial cells both within and downstream of the stent, is affected by the nature and extent of stent-induced flow disturbance. In this paper, we perform computational simulations that quantify the flow field and drug concentration in the vicinity of stents. We evaluate the effect of stent design by considering three different designs that resemble certain commercial closed-cell stent designs as well as three more simple and idealized designs that we have devised in order to develop a more complete understanding of the role of strut design. We also introduce the notion of “Stent Penalty Index” (SPI) which provides a quantitative measure of the penalty in stent performance incurred by the combination of stent-induced flow disturbance and endothelial-surface drug concentration.

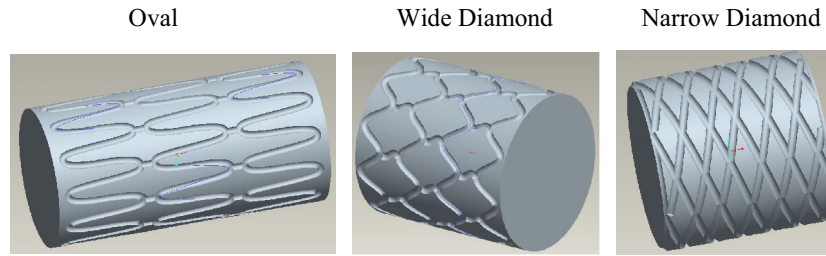
METHODS

Computational Models and Simulations

We have applied our computational analysis to the following three models that can be thought of as representative of some closed-cell commercial stent designs: (1) an elongated oval-shape cell design (henceforth referred to as “Oval”), (2) a wide diamond-shape cell design (“Wide Diamond”), and (3) a narrow diamond-shape cell design (“Narrow Diamond”). The effects of somewhat similar stent designs on the arterial flow field and on platelet deposition have previously been investigated^{11,12}; however, the impact on the concentration of drugs eluted by these stents is unknown. In addition to these stent designs, we also considered three more simple and idealized stent designs inspired by our previous investigations of stent-induced flow disturbance^{4,41}: a “ring” stent, a spiral stent, and an intertwined ring stent. Figure 1 depicts the six stent designs studied. In the simulations, we have considered stent strut cross-sections that are either circular with a diameter of 100 μm or square 100 μm to a side. These shapes and sizes are representative of modern stents. In all cases, the stents are assumed to be deployed within a straight, rigid, and circular cross-section arterial segment with an inner diameter of 4 mm, a representative value for human coronary arteries. The computational meshes for the three closed-cell stent design models were constructed using Pro-E (PTC, Needham, MA), whereas those for the idealized models were generated using Gambit 2.0.4 (Fluent Inc., Lebanon, NH). Detailed geometric parameters characterizing the stent models simulated in this study are provided in Table 1.

The computations involve solving the three-dimensional Navier–Stokes and convection–diffusion equa-

Closed-Cell Stent Designs



Idealized Stent Designs

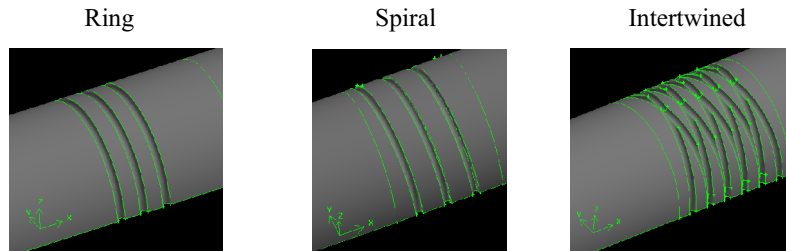


FIGURE 1. Stent designs simulated in the present study.

TABLE 1. Geometries of stents simulated in the present study.

	Stent design	Stent strut size (μm) ^a	Inter-strut distance (mm)	Total stent length (mm)
Closed-cell stent designs	Oval	100	4.68	8.0
	Wide Diamond	100	0.60	4.5
	Narrow Diamond	100	0.47	4.0
Idealized stent designs	Ring	100	0.4	1.4
	Spiral	100	0.60	2.8
	Intertwined	100	0.35	3.5

^aStent strut size is defined as the stent strut diameter for a circular cross-section strut and the length of a strut side for a square cross-section strut..

tions to determine the flow field and drug concentration in the vicinity of the model stents. Because the flow rate in coronary arteries remains nearly constant for a considerable portion of the cardiac cycle²¹ and since previous studies have suggested that the nature of flow disturbance in coronary arteries is similar for steady and pulsatile flow,² most of the results shown are for steady flow; however, unsteady flow simulations with a sinusoidal flow pulse were also performed for some of the geometries. The governing equations are as follows:

$$\text{Continuity: } \frac{\partial u_i}{\partial x_i} = 0 \quad (1)$$

$$\begin{aligned} \text{Linear momentum: } \rho \left[\frac{\partial u_i}{\partial t} + \frac{\partial (u_i u_j)}{\partial x_j} \right] \\ = - \frac{\partial p}{\partial x_i} + \mu \frac{\partial}{\partial x_j} \left(\frac{\partial u_i}{\partial x_j} \right) \end{aligned} \quad (2)$$

$$\text{Convection-diffusion: } \frac{\partial C}{\partial t} + u_i \frac{\partial C}{\partial x_i} = D \frac{\partial}{\partial x_i} \left(\frac{\partial C}{\partial x_i} \right), \quad (3)$$

where ρ , u_i , μ , and C , respectively denote blood density (1060 kg/m^3), blood velocity in the i direction (i runs from 1 to 3), blood dynamic viscosity (0.0035 Pa s), and drug concentration. D is the drug diffusion coefficient in blood and is taken to have a value of $1.4 \times 10^{-10} \text{ m}^2/\text{s}$, within the range considered elsewhere.²⁸ The assumption of constant blood viscosity, *i.e.* Newtonian behavior, is valid because shear rates in coronary arteries exceed the 100 s^{-1} threshold above which blood behaves as a Newtonian fluid. The governing equations were solved using the commercial software package FLUENT 6.3.2 (Fluent Inc., Lebanon, NH). The second-order upwind scheme was used to discretize the velocity and drug concentration variables using the Semi-Implicit Method for Pressure-

Linked Equation (SIMPLE) algorithm. The convergence tolerance for the continuity and velocity residuals was set at 10^{-5} . The boundary conditions were as follows: a uniform velocity profile and zero drug concentration at the inlet, zero pressure and zero drug concentration gradient at the outlet, no-slip (zero velocity) at all solid surfaces (arterial wall and stent surface), zero drug concentration gradient on the non-stented portion of the arterial wall, and a constant drug concentration $C_0 = 140 \mu\text{g}/\text{cm}^2$ at the stented portion of the arterial wall (*i.e.* the stent surface).⁴² Inlet flow rates corresponding to Reynolds numbers (*Re*) of 200, 400, and 800 were investigated. This range is representative of *in vivo* values present in the coronary vasculature.^{2,17} In the unsteady flow simulations, the imposed inlet velocity was a non-reversing sinusoidal waveform with a physiological frequency of 1 Hz and corresponding to a time-average Reynolds number of 200; thus, the imposed waveform was:

$$Re_{\text{in}} = 200[1 + 0.5 \sin(2\pi t)]. \quad (4)$$

Stent Penalty Index (SPI)

As already described, it is desirable to minimize both stent-induced flow disturbance and drug concentration at the endothelial surface. The drug concentration at the endothelial surface is computed directly in the simulations. To assess the extent of stent-induced flow disturbance, we compute the deviation in wall shear stress in the presence of a stent from the value that would be present in the absence of a stent (τ_{ns}). For steady, fully developed flow in a rigid tube of radius R , $\tau_{\text{ns}} = 4\mu\bar{U}/R$, where \bar{U} is the average flow velocity in the tube. To quantify the penalty in stent performance incurred by both stent-induced flow disturbance and drug concentration at the endothelial surface, we introduce a dimensionless quantity which we denote as the ‘‘Stent Penalty Index’’ (SPI) and define as:

$$\text{SPI} \equiv 0.5 \underbrace{\left(\frac{|\tau_w - \tau_{\text{ns}}|}{|\tau_{\text{max}} - \tau_{\text{ns}}|} \right)}_{\text{SPI}_\tau} + 0.5 \underbrace{\left(\frac{C}{C_0} \right)}_{\text{SPI}_C}, \quad (5)$$

where τ_w denotes the wall shear stress at any point within the region of interest and τ_{max} denotes the maximum wall shear stress within that region. The SPI has two components: SPI_τ which captures the effect of stent-induced flow disturbance and SPI_C which captures the effect of drug concentration at the endothelial surface. The two effects are assumed to be additive and equally weighted (as evi-

dent by the 0.5 coefficient multiplying each term), and their sum is the overall SPI. As defined, $0 \leq \text{SPI}_\tau \leq 0.5$, $0 \leq \text{SPI}_C \leq 0.5$, and $0 \leq \text{SPI} \leq 1$, with lower values corresponding to more desirable stent designs. It should be noted that the formulation provided in Eq. (5) is sufficiently general so that the weighting factors can be adjusted if necessary and additional terms that may be deemed important for stent performance can be added as desired.

RESULTS

Mesh Independence

To establish mesh independence of our numerical results, we have tested a wide range of mesh densities. A typical mesh used in generating the results consists of 2.2–2.3 million mesh points. At this density, the deviation in wall shear stress and wall concentration values relative to a finer mesh are smaller than 1%.

Penalty Indices of Commercial Stents

Figure 2 depicts contours of SPI_τ , SPI_C , and SPI in the stented portion of the artery for the three closed-cell stent designs studied with 100 μm -diameter circular cross-section struts and a $Re = 200$. For all stent models, there is a band bordering the stent struts where both the SPI_τ and SPI_C (and hence the SPI) exhibit relatively large values. The large SPI_τ values in this region are attributable to flow disturbance in the form of flow separation and recirculation immediately upstream and downstream of the stent struts as described in previous studies,^{17,37,41} and these regions are associated with higher drug concentrations, leading to elevated SPI_C values. As one moves away from the struts, the SPI_τ decreases in all stent models, although, because of its geometric design, the area of decreased SPI_τ is smaller for the Narrow Diamond stent than for the other two closed-cell designs. In the case of the SPI_C , the values are highest, not surprisingly, in the immediate vicinity of the struts and decrease as one moves away from the struts.

As the contour plots in Fig. 2 suggest, the average in-stent SPI_τ values are lower for the Oval and Wide Diamond designs than for the Narrow Diamond design, suggesting that the Narrow Diamond design disturbs the flow field to a greater degree than the other two designs. The in-stent SPI_C contours show that the Narrow Diamond design also leads to the highest drug concentration at the luminal surface. These findings are not surprising in light of the fact that the fraction of the total surface area occupied by struts is largest for the Narrow Diamond design. Interestingly, the Narrow Diamond design leads to ‘‘hot spots’’ of drug concentration at some of the strut junctions or cross-

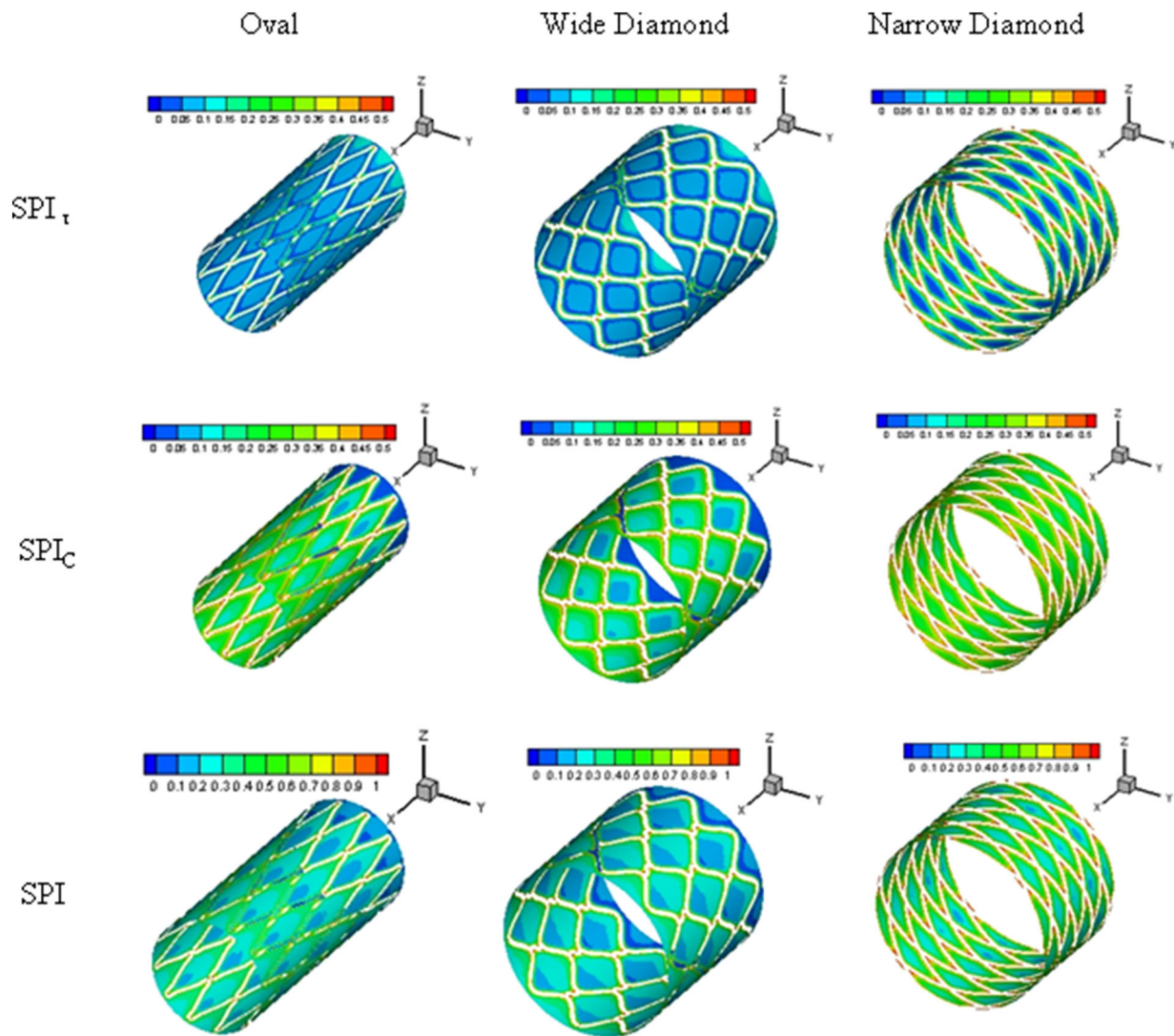


FIGURE 2. Contours of SPI_{τ} , SPI_C , and SPI for the three closed-cell stent designs. The stent struts have a circular cross-section with a diameter of $100 \mu\text{m}$. $Re = 200$.

ings; this effect appears to be largely absent in the other two designs. The SPI contours, which combine the effects of flow disturbance and concentration, naturally indicate that the Narrow Diamond design is associated with the highest and lowest SPI values, respectively.

The contour plots in Fig. 2 focus exclusively on the in-stent region and are only for $Re = 200$. Stents induce significant flow disturbance downstream of the stent,^{17,37,41} and this disturbance is expected to influence drug concentration at the luminal surface downstream of the stent. Therefore, we also examined the post-stent region in our simulations and quantified the values of SPI_{τ} , SPI_C , and SPI in this region. Figure 3 provides the average values of SPI_{τ} , SPI_C , and SPI for the three closed-cell stent designs with $100 \mu\text{m}$ -diameter circular cross-section struts and for both the in-stent and post-stent regions at Reynolds numbers of 200, 400, and 800.

The “average” values are defined as the average over the surface areas under consideration, and the post-stent region is defined as the entire computational domain downstream of the stent (a length of two vessel diameters). This choice of post-stent region does not influence the conclusions; a smaller post-stent length (one half of a vessel diameter) leads to the same behavior as that described here. The results indicate that the SPI_{τ} generally increases with Reynolds number, indicating increased levels of flow disturbance at the higher Reynolds numbers. Interestingly, this increase occurs primarily in the in-stent region for the Oval and Wide Diamond designs but mostly in the post-stent region for the Narrow Diamond design. The SPI_C in both the in-stent and post-stent regions decreases with Reynolds number for all designs. This result is not surprising as higher Reynolds numbers are associated with increased

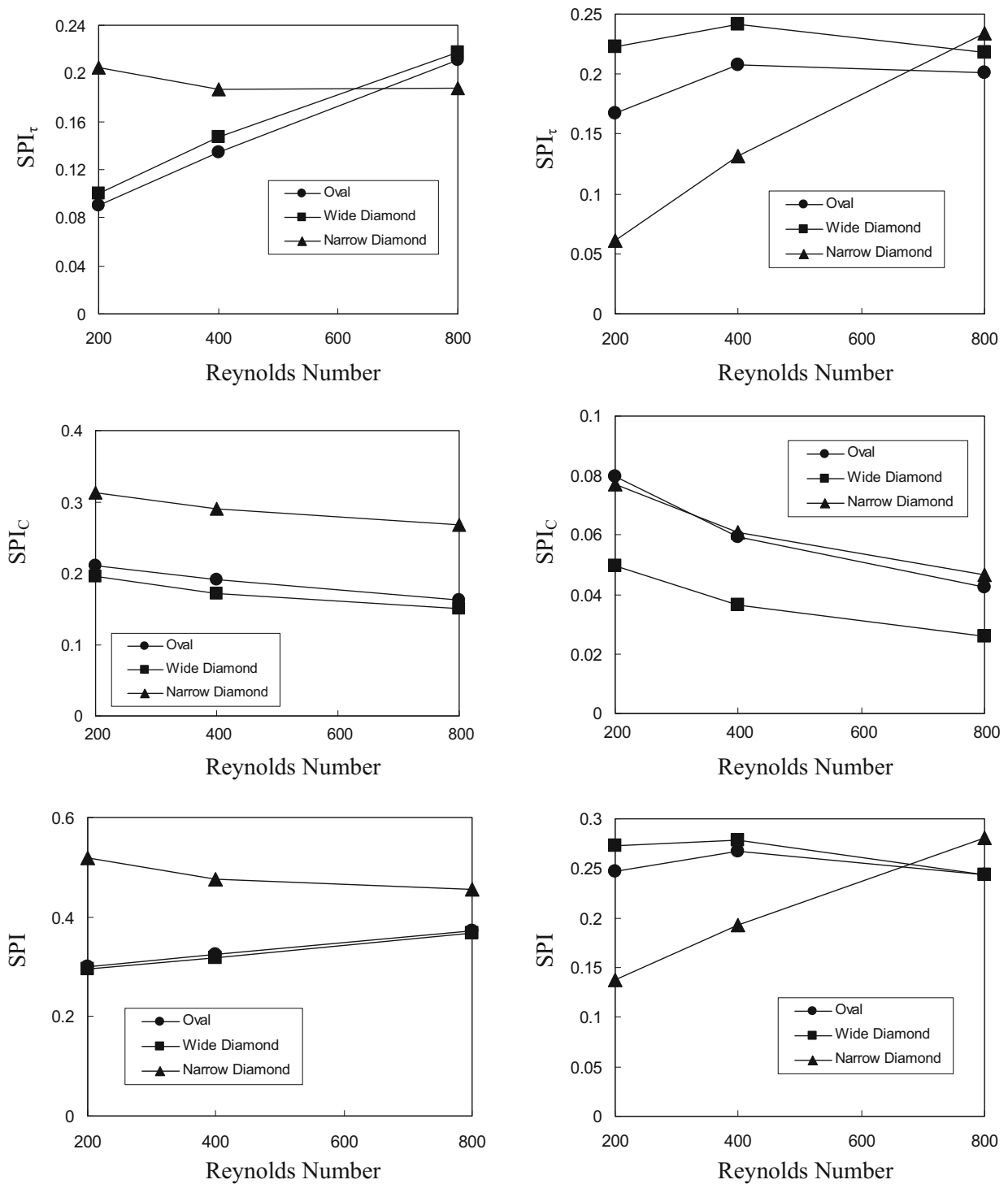


FIGURE 3. Dependence of the average SPI_{τ} , SPI_C , and SPI on Reynolds number in both the in-stent and post-stent regions for the three closed-cell stent designs. The post-stent region is defined as the entire computational domain downstream of the stent. Data are for circular cross-section struts with a diameter of $100 \mu\text{m}$.

convection which leads to higher rates of drug washout and consequently to lower drug concentrations at the endothelial surface.

Figure 3 also reveals significant differences among the three stent designs. In the in-stent region, the

Narrow Diamond design suffers from higher values of SPI_{τ} and SPI_C (and hence SPI) than the other two designs for most of the Reynolds numbers studied. The Oval and Wide Diamond designs exhibit largely similar values of in-stent SPI_{τ} and SPI_C . In the post-stent

region, the Narrow Diamond design is associated with the lowest values of SPI overall; this effect is driven primarily by the apparent advantage of this design in terms of the SPI_{τ} . Interestingly, in most cases and in both the in-stent and post-stent regions, the opposite dependence on Reynolds number of SPI_{τ} and SPI_C leads to a relatively weak dependence of the SPI on Reynolds number, which suggests a level of robustness of these designs.

Because, as Fig. 3 shows, the dependence of the SPI_{τ} on Reynolds number in both the in-stent and post-stent regions is the opposite of that of the SPI_C , the relative contributions of flow disturbance and endothelial cell drug concentration to the overall degradation of stent performance change with Reynolds number. Furthermore, there are differences in this regard among the different stent designs. Figure 4 depicts the SPI_C -to- SPI_{τ} ratio in both the in-stent and post-stent regions for the three closed-cell stent designs studied and for the same conditions described in

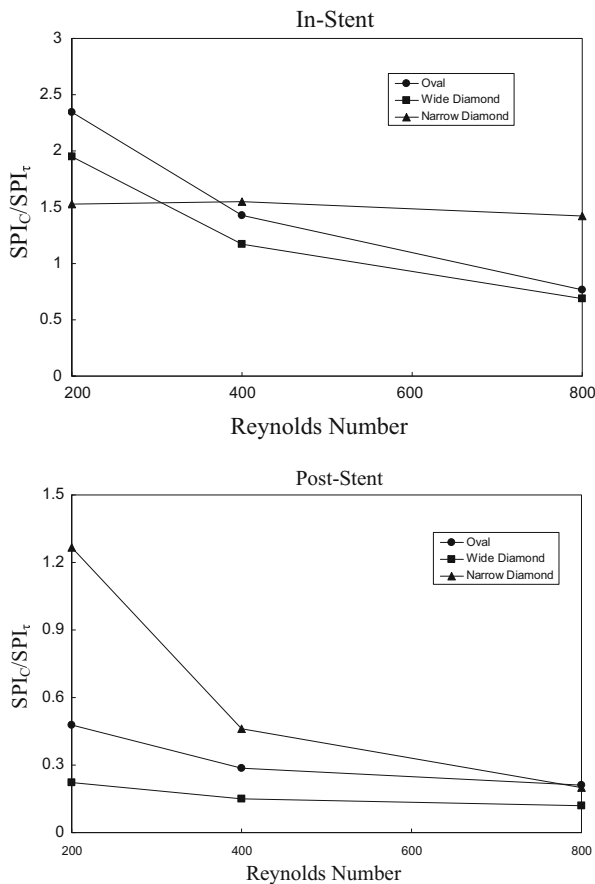


FIGURE 4. Dependence of the SPI_C -to- SPI_{τ} ratio on Reynolds number in both the in-stent and post-stent regions for the three closed-cell stent designs. The post-stent region is defined as the entire computational domain downstream of the stent. Data are for circular cross-section struts with a diameter of $100 \mu\text{m}$.

Fig. 3. For both the Oval and Wide Diamond designs, this ratio is considerably larger in the in-stent region than in the post-stent region, suggesting that whereas retarded wound healing in the in-stent region is dominated more by the effect of the drug concentration at the endothelial surface, the relative contribution of flow disturbance increases in the post-stent region. In the case of the Narrow Diamond design, the differences between the in-stent and post-stent regions are not as stark. The SPI_C -to- SPI_{τ} ratio decreases with Reynolds number in both the in-stent and post-stent regions, reflecting the combined effects of increased flow disturbance and reduced drug concentration at the endothelial surface as the Reynolds number increases. In the in-stent region, the sensitivity of the SPI_C -to- SPI_{τ} ratio to Reynolds number is smallest for the Narrow Diamond design, suggesting that although this design suffers from relatively elevated SPI values, its performance is generally less sensitive to changes in blood flow than the other two stent designs.

Effect of Stent Strut Shape

The results thus far were for stents of circular cross-section struts. Many stents in use today have square cross-section struts; therefore, we performed simulations for the Wide Diamond and Narrow Diamond designs with square cross-section struts $100 \mu\text{m}$ to a side. The SPI results of these simulations for both the in-stent and post-stent regions are shown in Fig. 5. Comparison of these results with those in Fig. 3 reveals that the strut shape has a minimal impact on the SPI in the in-stent region. In the post-stent region, however, while the SPI values for the square and circular struts are largely similar for the Narrow Diamond design, they are somewhat lower for the square struts than for the circular struts in the case of the Wide Diamond design, particularly at the lower Reynolds numbers.

Effect of Flow Unsteadiness

All the results thus far assumed steady flow. To explore the effect of flow unsteadiness, we performed a number of unsteady flow simulations. In these simulations, the imposed flow at the inlet was a non-reversing sinusoid with a physiological frequency of 1 Hz and a cycle-average Reynolds number of 200 (see Eq. 4 above). Figure 6 depicts the evolution of SPI during the pulsatile cycle in both the in-stent and post-stent regions for the Oval, Wide Diamond, and Narrow Diamond designs with $100 \mu\text{m}$ -diameter circular cross-section struts. The results suggest relatively mild variations during the pulsatile cycle in the in-stent region but larger fluctuations in the post-stent region. In the in-stent region, the time-average SPI values for un-

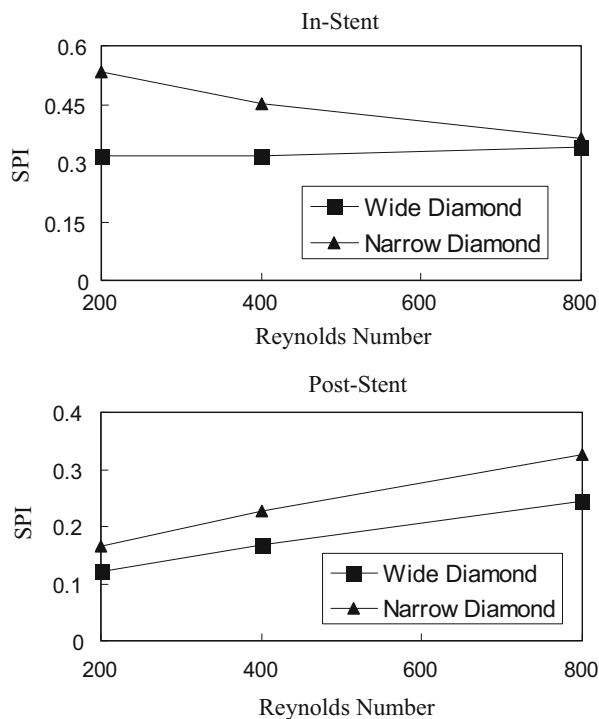


FIGURE 5. Dependence of the SPI on Reynolds number in both the in-stent and post-stent regions for the Wide Diamond and Narrow Diamond stent designs. The post-stent region is defined as the entire computational domain downstream of the stent. Data are for square cross-section struts $100\ \mu\text{m}$ to a side.

steady flow are somewhat higher than those obtained for steady flow at $Re = 200$ (cf: Fig. 3); however, this difference is largely absent in the post-stent region.

Penalty Indices of Idealized Stent Designs

In order to better understand the dependence of in-stent and post-stent flow disturbance and endothelial cell surface drug concentration on specific features of stent design, we developed three simple, “idealized” stent designs and computed the penalty indices associated with these designs. The idealized designs, illustrated in Fig. 1, were as follows: (1) a “ring” stent that consists simply of a series of rings with no inter-ring connections, (2) a “spiral” stent, and (3) an “intertwined ring” stent, consisting of six rings that intersect at a fixed angle of 30° . The ring stent allows determination of the effect of stent struts *per se* on the penalty indices, the spiral stent additionally permits examination of the effect of the simplest form of inter-strut connection, and the intertwined stent further allows determination of the effect of strut intersections. In all cases, the struts had a circular cross-section, and the strut diameters and inter-strut spacings were largely similar to those used in the closed-cell stent design simulations.

Figure 7 depicts the average values of SPI_r , SPI_C , and SPI for the three idealized stent designs (stent strut diameter of $100\ \mu\text{m}$) and for both the in-stent and post-stent regions at Reynolds numbers of 200, 400, and 800. Generally speaking, the spiral stent leads to the lowest values of all indices in both the in-stent and post-stent regions for all Reynolds numbers. Comparison of Figs. 3 and 7 reveals that in the in-stent region, the spiral stent exhibits largely similar SPI behavior to the Oval and Wide Diamond designs. Therefore, these stent models are expected to be the stent designs that most minimally disturb the flow field while also leading to the lowest drug concentration at the endothelial cell surface. In many of the cases considered, the performance of the Ring stent in the in-stent region is somewhat similar to that of the Narrow Diamond design.

DISCUSSION

Sufficiently rapid endothelial wound healing is essential for preventing restenosis and thrombosis following deployment of an endovascular stent. In addition to biochemical factors, biomechanical factors including stent-induced blood flow disturbance and resulting fluid mechanical shearing stresses influence endothelial cell wound repair^{1,15,16}. In the case of DES, the eluted drug may additionally act on endothelial cells and slow down their wound healing capacity.^{34,45} In this study, we performed computational simulations to explore how the design of DES affects both the flow field in the vicinity of the stent as well as the concentration of the eluted drug at the endothelial cell surface. Simulations were performed on three geometries that resemble some commercial closed-cell stent designs. In addition, simulations were performed on three idealized stent models that we developed in order to better understand the role of aspects of stent geometry on the flow field and eluted drug concentration.

To provide an objective basis for quantitative comparisons among the different stent designs, we introduced the notion of the SPI, a dimensionless quantity that incorporates the effects of both stent-induced flow disturbance (SPI_r) and endothelial cell surface drug concentration (SPI_C). The SPI is formulated in such a manner that its value is always between 0 and 1 with lower values corresponding to superior stent performance. It is recognized, of course, that simple superposition of the effects of flow disturbance and drug concentration used here is somewhat arbitrary; however, in the absence of more detailed information on how these two factors combine, the approach taken here appears reasonable.

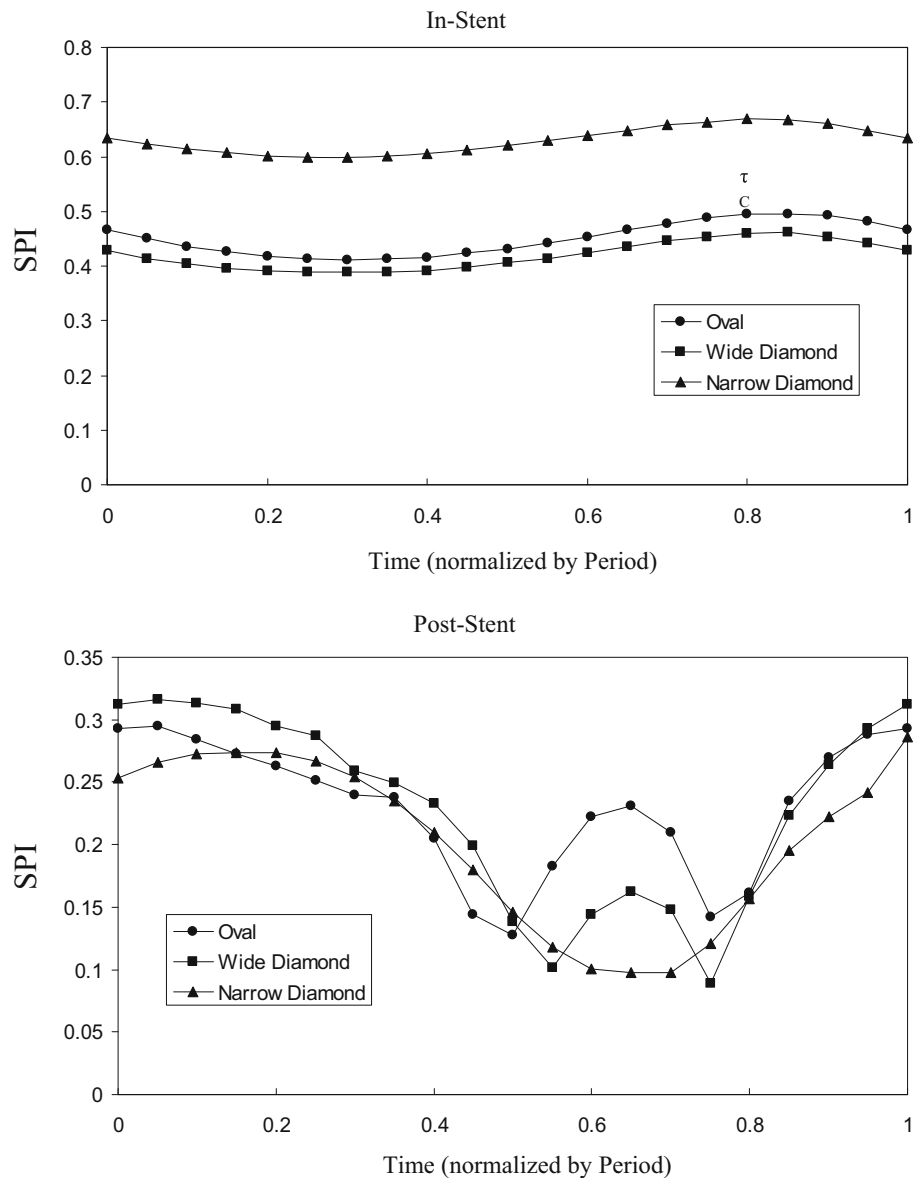


FIGURE 6. Time evolution of SPI in both the in-stent and post-stent regions for the Oval, Wide Diamond, and Narrow Diamond designs in pulsatile flow. The flow waveform is a non-reversing sinusoid with a physiological frequency of 1 Hz and a time-average Reynolds number of 200. Data are for circular cross-section struts with a diameter of 100 μm .

Our results have demonstrated that consistent with our previous work and that of others,^{4,5,11,17,41} stents induce significant disturbance of the local flow field. This disturbance, which takes the form of flow separation zones both within and immediately upstream and downstream of the stent, leads to a highly heterogeneous wall shear stress environment. In turn, this flow disturbance affects interactions between the drug eluted into the bloodstream and the underlying endothelium. Therefore, through its effect on the local flow environment, stent design also affects the concentration of eluted drug to which endothelial cells are exposed.

Among the three closed-cell stent designs studied, our simulations have revealed that the Oval and Wide Diamond designs are associated with lower in-stent SPI values than the Narrow Diamond design. This finding is probably attributable to the fact that the Narrow Diamond design is associated with a higher stent-to-artery area ratio than the other two designs, and it suggests that the Oval and Wide Diamond designs provide a more hemodynamically favorable environment for the range of flow Reynolds numbers studied ($200 \leq Re \leq 800$) than the Narrow Diamond design. These results suggest that in-stent endothelial wound healing would be expected to occur more effi-

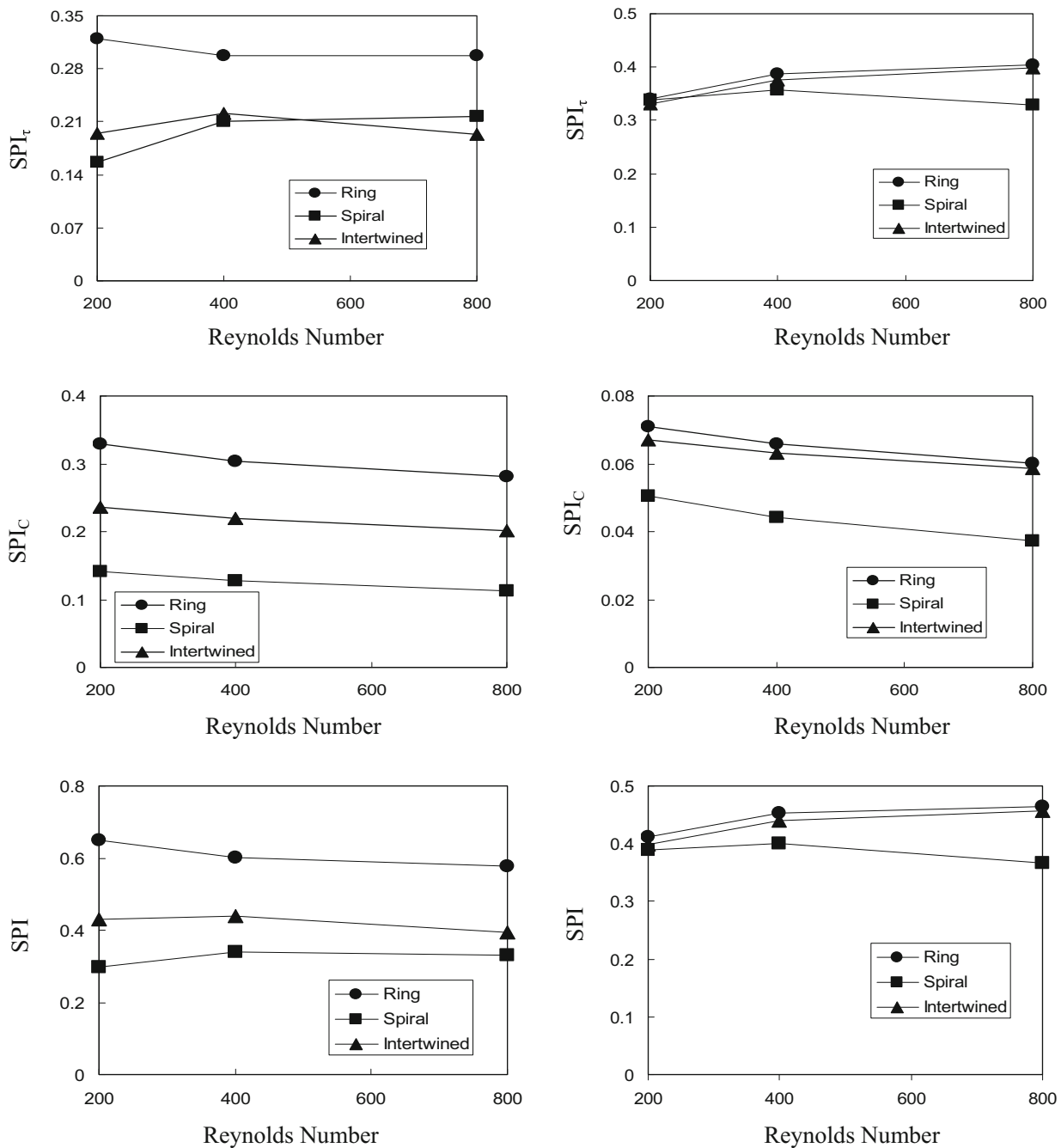


FIGURE 7. Dependence of the average SPI_t, SPI_c, and SPI on Reynolds number in both the in-stent and post-stent regions for the three idealized stent designs. The post-stent region is defined as the entire computational domain downstream of the stent. Data are for circular cross-section struts with a diameter of 100 μm.

ciently for the Oval and Wide Diamond designs than for the Narrow Diamond design. In the post-stent region, the SPI values for the Narrow Diamond design are lower than those for the Oval and Wide Diamond designs at lower Reynolds numbers, but these values increase rapidly as the Reynolds number increases. Overall, when both the in-stent and post-stent regions are considered, the Wide Diamond design would be

predicted to be preferable from the perspective of hemodynamics and vascular re-endothelialization to the Narrow Diamond design. These findings are largely consistent with those of Duraiswamy et al.¹² that have demonstrated smaller low-shear (<0.5 Pa) zones with the BX Velocity stent (whose design resembles the Wide Diamond design considered here) than the Wallstent (which resembles the Narrow Diamond design).

In addition to the closed-cell stent designs, we computed the SPI for three idealized stent designs and determined that a spiral stent provides particularly favorable performance (low SPI) under all flow conditions investigated. In contrast, stents consisting of a series of rings or containing many strut intersections such as the intertwined design considered here are associated with higher SPI and are thus less favorable from the perspective of hemodynamics and the consequent effect on eluted drug concentration.

To our knowledge, no systematic comparison has been performed to date of the performance of different stent designs in terms of endothelial wound healing; therefore, the predictions of our simulations remain to be experimentally validated. It is recognized, of course, that *in vivo*, endothelial wound healing rates following the deployment of DES are determined by other factors in addition to the local flow environment and the concentration of the eluted drug at the endothelial surface. As such, the concept of the SPI as formulated in the present study remains incomplete. However, an advantage of the SPI formulation in addition to its simplicity is that it is “modular” so that additional factors can be added to the present formulation as desired.

Because the results of any model depend fundamentally on the assumptions under which the model is formulated, it is important to address the general validity of the assumptions used in the simulations. In most of the simulations, we have assumed blood flow to be steady. Although flow in the coronary arteries *in vivo* is unsteady, the flow rate is fairly constant over a significant portion of the cardiac cycle.²¹ Furthermore, previous studies of flow in coronary arteries have suggested that the nature of flow disturbance is similar for steady and pulsatile flow,² so that the general conclusions drawn here are expected to remain valid. The unsteady flow simulations performed here generally support this assertion, and the time-average SPI values are found to be somewhat higher than but not all that different from their steady flow counterparts. On the other hand, flow unsteadiness led to significant fluctuations in the post-stent SPI during the course of the pulsatile cycle.

We have also assumed the stents to be deployed in straight and rigid-wall arterial segments. Vessel curvature introduces secondary flow motion, and these secondary flows may have significant effects on the size of flow disturbance zones as well as the resulting wall shear stress. The effect of arterial wall compliance on the detailed flow field remains controversial and is a subject of active study.^{14,18,43} While some studies have reported wall motion to have a signifi-

cant effect on the flow field, other studies have suggested otherwise. In any case, the effects of curvature and wall compliance merit further study in future investigations.

Additional factors that might be expected to impact the present findings include the extent of stent embedment within the arterial wall upon deployment as well as stent malapposition if it occurs. The effect of the extent of stent embedment would be expected to resemble to some degree the effect of changing the stent strut size; thus, higher embedment would be expected to lead to lower flow disturbance (and hence lower SPI_{τ}) and to lower SPI_C as more of the drug goes into the arterial wall rather than into the lumen. Stent malapposition would be expected to lead to higher SPI_{τ} values due to increased flow disturbance but to lower values of SPI_C as a smaller portion of the stent would be in direct contact with the arterial wall. Thus, the effect of stent malapposition on overall SPI would depend on how large the SPI_{τ} effect is relative to that of SPI_C .

One rather obvious implication of the present work is that it is preferable to coat stents with drugs only on their abluminal (external) surface, and this is indeed the case in some of the latest-generation commercial DES. However, many of the DES in commercial use today remain coated along their entire surface; therefore, the current findings remain relevant. It should be noted in this regard that although the fraction of total stent drug loading released into the lumen is not known, drugs used in DES are much more soluble in lipid than in water. However, in light of the lipid content of blood, some drug release into the lumen would be expected nevertheless.

Finally, it is recognized that in addition to its effect on flow disturbance and endothelial cell drug concentration, the process of stent design involves a number of other considerations including structural stability, stent flexibility, ease of deployment, *etc.* These considerations were not accounted for in the present study. In principle, future studies can build on the present results by incorporating into the SPI concept additional biochemical and biophysical considerations that may affect stent performance.

ACKNOWLEDGMENTS

TS was supported in part by Basic Science Research Program through the National Research Foundation of Korea (NRF), Korea. This work was funded in part by an endowment in Cardiovascular Cellular Engineering from the AXA Research Fund.

DISCLOSURES

None.

REFERENCES

- ¹Albuquerque, M. C., C. M. Waters, U. Savla, H. W. Schnaper, and A. S. Flozak. Shear stress enhances human endothelial cell wound closure in vitro. *Am. J. Physiol.* 279:H293–H302, 2000.
- ²Asakura, T., and T. Karino. Flow patterns and spatial distribution of atherosclerotic lesions in human coronary arteries. *Circ. Res.* 66:1045–1066, 1990.
- ³Balossino, R., F. Gervaso, F. Migliavacca, and G. Dubini. Effects of different stent designs on local hemodynamics in stented arteries. *J. Biomech.* 41:1053–1061, 2008.
- ⁴Barakat, A. I. and Cheng, E. T. Numerical simulation of fluid mechanical disturbance induced by intravascular stents. In: Proceedings of the 11th international conference on mechanical, medicine and biology, pp. 33–36, 2000.
- ⁵Berry, J. L., A. Santamarina, J. E. Moore, S. Roychowdhury, and W. D. Routh. Experimental and computational evaluation of coronary stent. *Ann. Biomed. Eng.* 28:386–398, 2000.
- ⁶Bozsak, F., J. Chomaz, and A. I. Barakat. Modeling transport of drugs eluted from stents: physical phenomena driving drug distribution in the arterial wall. *Biomech. Model. Mechanobiol.* 13:327–347, 2014.
- ⁷Camenzind, E. Treatment of in-stent restenosis—back to the future? *N. Engl. J. Med.* 355:2149–2151, 2006.
- ⁸Coppola, G., and C. Caro. Arterial geometry, flow pattern, wall shear and mass transport: potential physiological significance. *J. R. Soc. Interface* 6:519–528, 2009.
- ⁹Davies, P. F., A. Remuzzi, E. J. Gordon, C. F. Dewey, and M. A. Gimbrone. Turbulent fluid shear stress induces vascular endothelial cell turnover in vitro. *Proc. Natl. Acad. Sci. USA* 83:2114–2117, 1986.
- ¹⁰Depaola, N., M. A. Gimbrone, P. F. Davies, and C. F. Dewey. Vascular endothelium responds to fluid shear stress gradients. *Arterioscler. Thromb. Vasc. Biol.* 12:1254–1257, 1992.
- ¹¹Duraiswamy, N., J. M. Cesar, R. T. Schoepfoerster, and J. E. Moore. Effects of stent geometry on local flow dynamics and resulting platelet deposition in an in vitro model. *Biorheology* 45:547–561, 2008.
- ¹²Duraiswamy, N., R. T. Schoepfoerster, and J. E. Moore. Comparison of near-wall hemodynamic parameters in stented artery models. *J. Biomech. Eng.* 131:061006, 2009.
- ¹³Finn, A. V., G. Nakazawa, M. Joner, F. D. Kolodgie, E. K. Mont, H. K. Gold, and R. Virmani. Vascular responses to drug eluting stents: importance of delayed healing. *Arterioscler. Thromb. Vasc. Biol.* 27:1500–1510, 2007.
- ¹⁴Gerbeau, J., M. Vidrascu, and P. Frey. Fluid-structure interaction in blood flows on geometries based on medical imaging. *Compos. Struct.* 83:155–165, 2005.
- ¹⁵Gojova, A., and A. I. Barakat. Vascular endothelial wound closure under shear stress: role of membrane fluidity and flow-sensitive channels. *J. Appl. Physiol.* 98:2355–2362, 2005.
- ¹⁶Hsu, P. P., S. Li, Y. S. Li, S. Usami, A. Ratcliffe, X. Wang, and S. Chien. Effects of flow patterns on endothelial cell migration into a zone of mechanical denudation. *Biochem. Biophys. Res. Commun.* 285:751–759, 2001.
- ¹⁷Jimenez, J. M., and P. F. Davies. Hemodynamically driven stent strut design. *Ann. Biomed. Eng.* 37:1483–1494, 2009.
- ¹⁸Jin, S., J. Oshinski, and D. P. Giddens. Effects of wall motion and compliance on flow patterns in the ascending aorta. *J. Biomech. Eng.* 125:347–354, 2005.
- ¹⁹Kastrati, A., J. Mehilli, J. Dirschinger, F. Dotzer, H. Schühlen, F. J. Neumann, M. Fleckenstein, C. Pfafferoth, M. Seyfarth, and A. Schömig. Intracoronary stenting and angiographic results: strut thickness effect on restenosis outcome (ISAR-STERO) trial. *Circulation* 103:2816–2821, 2001.
- ²⁰Kastrati, A., J. Mehilli, J. Dirschinger, J. Pache, K. Ulm, H. Schühlen, M. Seyfarth, C. Schmitt, R. Blasini, F. J. Neumann, and A. Schömig. Restenosis after coronary placement of various stent types. *Am. J. Cardiol.* 87:34–39, 2001.
- ²¹Kim, H. J., I. E. Vignon-Clmentel, J. S. Coogan, C. A. Figueroa, J. E. Jansen, and C. A. Taylor. Patient-specific modeling of blood flow and pressure in human coronary arteries. *Ann. Biomed. Eng.* 38:3195–3209, 2010.
- ²²LaDisa, J. F., L. E. Olson, I. Guler, D. A. Hettrick, J. R. Kersten, D. C. Warltier, and P. S. Pagel. Stent design properties and deployment ratio influence indexes of wall shear stress: a three-dimensional computational fluid dynamics investigation within a normal artery. *J. Appl. Physiol.* 97:424–430, 2004.
- ²³Luscher, T. F., J. Steffel, F. R. Eberli, M. Joner, G. Nakazawa, F. C. Tanner, and R. Virmani. Drug-eluting stent and coronary thrombosis: biological mechanisms and clinical implications. *Circulation* 115:1051–1058, 2007.
- ²⁴McGinty, S. A decade of modelling drug release from arterial stents. *Math. Biosci.* 257:80–90, 2014.
- ²⁵McGinty, S., S. McKee, R. M. Wadsworth, and C. McCormick. Modelling drug-eluting stents. *Math. Med. Biol.* 28:1–29, 2011.
- ²⁶McGinty, S., T. N. Vo Tuoi, M. Meere, and Mc Cormick C. McKee. Some design considerations for polymer-free drug-eluting stents: a mathematical approach. *Acta Biomater.* 18:213–225, 2015.
- ²⁷Miyazaki, S., Y. Hiasa, T. Takahashi, Y. Yano, T. Minami, N. Murakami, M. Mizobe, Y. Tobetto, T. Nakagawa, P. M. Chen, R. Ogura, H. Miyajima, K. Yuba, S. Hosokawa, K. Kishi, and R. Ohtani. In vivo optical coherence tomography of very late drug-eluting stent thrombosis compared with late in-stent restenosis. *Circ. J.* 76:390–398, 2012.
- ²⁸Mongrain, R., I. Faik, R. L. Leask, J. R. Cabau, E. Larose, and O. F. Bertrand. Effects of diffusion coefficients and struts apposition using numerical simulations for drug eluting coronary stents. *J. Biomech. Eng.* 129:733–742, 2007.
- ²⁹Morton, A. C., D. Crossman, and J. Gunn. The influence of physical stent parameters upon restenosis. *Pathol. Biol.* 52:196–205, 2004.
- ³⁰Moses, J. W., M. B. Leon, J. J. Popma, P. J. Fitzgerald, D. R. Holmes, C. O’Shaughnessy, R. P. Caputo, D. J. Keriaikes, D. O. Williams, P. S. Teirstein, J. L. Jaeger, and R. E. Kuntz. Sirolimus-eluting stent versus standard stents in patients with stenosis in a native coronary artery. *N. Engl. J. Med.* 349:1315–1323, 2003.
- ³¹Ong, A. T., E. P. McFadden, E. Regar, P. P. de Jaegere, R. T. van Domburg, and P. W. Serruys. Late angiographic stent thrombosis (LAST) events with drug-eluting stents. *J. Am. Coll. Cardiol.* 45:2088–2092, 2005.

- ³²Pache, J., J. Kastrati, H. Mehilli, H. Schühlen, F. Dotzer, J. Hausleiter, M. Fleckenstein, F. J. Newmann, U. Sattler, C. Schmitt, M. Müller, J. Dirschinger, and A. Schömig. Intracoronary stenting and angiographic results: strut thickness effect on restenosis outcome (ISAR-STE-REO-2) trial. *J. Am. Coll. Cardiol.* 41:1283–1288, 2003.
- ³³Pant, S., N. W. Bressloff, A. I. J. Forrester, and N. Curzen. The influence of strut-connectors in stented vessels: a comparison of pulsatile flow through five coronary stents. *Ann. Biomed. Eng.* 38:1893–1907, 2010.
- ³⁴Parry, T. J., R. Brosius, R. Thyagarajan, D. Carter, D. Argentieri, R. Falotico, and J. Siekierka. Drug-eluting stents: sirolimus and paclitaxel differentially affect cultured cells and injured arteries. *Eur. J. Pharmacol.* 524:19–29, 2005.
- ³⁵Pfisterer, M., H. P. Brunner-La Rocca, P. T. Buser, P. Rickenbacher, P. Hunziker, C. Mueller, R. Jeger, F. Bader, S. Osswald, and C. Kaiser. Late clinical events after clopidogrel discontinuation may limit the benefit of drug-eluting stents: an observational study of drug-eluting versus bare-metal stents. *J. Am. Coll. Cardiol.* 48:2584–2591, 2006.
- ³⁶Pontrelli, G., and F. de Monte. A multi-layer porous wall model for coronary drug-eluting stents. *Int. J. Heat Mass Transf.* 53:3629–3637, 2010.
- ³⁷Rajamohan, D., R. K. Banerjee, L. H. Back, A. A. Ibrahim, and M. A. Jog. Developing pulsatile flow in a deployed coronary stent. *J. Biomech. Eng.* 128:347–359, 2006.
- ³⁸Rogers, C., and E. R. Edelman. Endovascular stent design dictates experimental restenosis and thrombosis. *Circulation* 91:2995–3001, 1995.
- ³⁹Rogers, C., C. Parikh, P. Seifert, and E. R. Edelman. Endogenous cell seeding—remnant endothelium after stenting enhances vascular repair. *Circulation* 94:2909–2914, 1996.
- ⁴⁰Sarno, G., B. Lagerqvist, O. Fröbert, J. Nilsson, G. Olivecrona, E. Omerovic, N. Saleh, D. Venetianos, and S. James. Lower risk of stent thrombosis and restenosis with unrestricted use of ‘new-generation’ drug-eluting stents: a report from the nationwide Swedish coronary angiography and angioplasty registry (SCAAR). *Eur. Heart J.* 33:606–613, 2012.
- ⁴¹Seo, T. W., L. G. Schachter, and A. I. Barakat. Computational study of fluid mechanical disturbance induced by endovascular stents. *Ann. Biomed. Eng.* 33:444–456, 2005.
- ⁴²Sousa, J. E., M. A. Costa, A. C. Abizaid, B. J. Rensing, A. S. Abizaid, L. F. Tanajura, K. Kozuma, G. V. Langenhove, A. G. Sousa, R. Falotico, J. Jaeger, J. J. Popma, and P. W. Serruys. Sustained suppression of neointimal proliferation by sirolimus-eluting stents. *Circulation* 104:2007–2011, 2001.
- ⁴³Tezduyar, T. E., S. Sathe, M. Schwaab, and B. S. Conklin. Arterial fluid mechanics modeling with stabilized space-time fluid-structure interaction technique. *Int. J. Numer. Methods Fluids* 57:601–629, 2008.
- ⁴⁴Tzafiriri, A. R., A. D. Levin, and E. R. Edelman. Diffusion-limited binding explains binary dose response for local arterial and tumour drug delivery. *Cell Prolif.* 42:348–363, 2009.
- ⁴⁵Van der Heiden, K., F. J. Gijzen, A. Narracott, S. Hsiao, I. Halliday, J. Gunn, J. J. Wentzel, and P. C. Evans. The effects of stenting on shear stress: relevance to endothelial injury and repair. *Cardiovasc. Res.* 99:269–275, 2013.
- ⁴⁶Wentzel, J. J., R. Krams, J. C. H. Schuurbers, J. A. Oomen, J. Kloet, W. J. van Der Giessen, P. W. Serruys, and C. J. Slager. Relationship between neointimal thickness and shear stress after Wallstent implantation in human coronary arteries. *Circulation* 103:1740–1745, 2001.